第33卷第5期
2014年10月

红外与毫米波学报
J. Infrared Millim. Waves

Vol. 33, No. 5
October, 2014

文章编号:1001-9014(2014)05-0465-07

DOI:10.3724/SP.J.1010.2014.00465

Vehicle detection based on vision and millimeter wave radar

JIN Lu[1,2], FU Meng-Yin[1,2*], WANG Mei-Ling[1,2], YANG Yi[1,2]

(1. School of Automation, Beijing institute of technology, Beijing 100081, China;
2. Key Laboratory of Intelligent Control and Decision of Complex Systems, Beijing 100081, China)

Abstract: With the importance of automotive drive assistance system of intelligent vehicle, vehicle detection fusing millimeter wave (MMW) radar data and vision multi-features is presented. The vehicle detection algorithm can be divided into three steps. Firstly, a space alignment algorithm between MMW radar and vision was proposed to get space alignment point according to the space transformation matrix of image coordinate and radar coordinate. The second step obtains region of interest (ROI) according to the space aligned point and search strategy. At last, vehicle detection was realized through features of vehicle including bottom shadow, symmetry, left and right edges; in this step, an improved segmentation algorithm of bottom shadow of vehicle was described in order to obtain accurate vehicle width. The performance of the algorithm was verified under different scenarios. The results show the vehicle detection algorithm is effective and feasible.

Key words: automotive driver assistance system, vehicle detection, space alignment, ROI, bottom shadow
PACS: 07.57.-c;42.30.-d

基于视觉和毫米波雷达的车辆检测

靳 璐[1,2], 付梦印[1,2*], 王美玲[1,2], 杨 毅[1,2]
(1. 北京理工大学 自动化学院,北京 100081;
2. 复杂系统智能控制与决策教育部重点实验室,北京 100081)

摘要:根据智能车辆主动驾驶辅助系统中的重要性,提出了一种融合毫米波雷达数据和视觉多特征的车辆检测算法。车辆检测算法通过三个步骤实现,首先,提出一种空间对准算法实现毫米波雷达和视觉的空间对准;其次,根据空间对准结果和搜索策略提取目标车辆的感兴趣区域;最后,融合车底阴影、对称轴、左右边缘等车辆特征实现车辆检测,其中,为了准确得到目标车辆的车底阴影,提出一种改进的车底阴影分割算法。算法的性能在不同的场景下得到证实,实验结果表明该车辆检测算法是有效和可靠的。

关 键 词:主动驾驶辅助系统;车辆检测;空间对准;感兴趣区域;车底阴影

中图分类号:TP242 **文献标识码**:A

Introduction

With the sharply growing of vehicle, the traffic accidents happen frequently and cause heavy casualties and financial losses. In order to improve the traffic security level, developing the automotive driver assistance systems has attracted a large amount of attention lately. The reliable vehicle detection becomes a very important aspect of automotive system[1].

The major advantage of radar-vision fusion benefits from the best performance of each sensor by fusing results from different sensors together[2]. MMW radar can detect moving vehicles fast and provide the long-range detection and exact velocity measurement. Nevertheless, vision can obtain the contour of vehicles in the short-range sensing region[3]. So radar-vision fusion based on complementary devices can provide an improved performance: improved reliability from multiple detections and the merging of position measurements with good longitudinal and lateral accuracy[4].

The radar-vision fusion approach mainly focuses on the space alignment of radar-vision sensors and the verification of radar target. The general space alignment algo-

Received date: 2013-10-17, **revised date**: 2014-07-03 **收稿日期**: 2013-10-17, **修回日期**: 2014-07-03
Foundation items: Supported by the Nation Science Foundation of China (91120003); Nation Science Foundation of China (61105092); Beijing Natural Science Foundation(4101001)
Biography: JIN Lu(1982-), male, Changzhi Shanxi, Ph D, Research area involves intelligent navigation and information fusion. E-mail: 10906009@bit.edu.cn
* **Corresponding author**: E-mail: fumy@bit.edu.cn

rithm is a complex task, because it needs to estimate the interior parameters of each senor and the exterior parameters between different sensors [5]. SUGIMOTO et al. [3] considered the position that has maximum reflection intensity from MMW radar as position of the target in image, and realized radar-vision space alignment. Nevertheless, the reflection intensity needs special tool to obtain and cannot be explained clearly. WANG et al. [6] utilized pairs of the corresponding points composed of the centroid of target and radar target to realize the space alignment without special tool and reflection intensity. However the range of space alignment is too small to be adapted for the intelligent vehicle with large speed. DENASI et al. [7] used the deformable models adding the detail of car to detect the vehicle. FLEISCHE et al. [8] took into consideration vehicle misalignment with the vision sensor and integrated 3D models to detect vehicle. Nevertheless, these methods need to match different vehicle types. ZIEKE et al. [9] utilized image intensity symmetry to locate the position of vehicle, but the result is prone to influences of illumination. HUANG et al. [10] made use of the left and right edges to verify the vehicle. KIM et al. [11] utilized the bottom shadow of vehicle for generating the ROI and the symmetry for verifying the existence of vehicle. TEOH et al. [12] used the center points of the symmetric regions clustered by the symmetric points to detect the vehicle. ALESSANDRETTI et al. [2] fused radar-vision information and employed symmetry of edges image to locate the position of vehicle, but the drawback of the technique is that it detects the global symmetry of the image. However, a single feature used to verify vehicle is very weak for reliable vehicle detection. Therefore, multiple vision features should be used and fused in order to obtain robust and reliable detection results. By investigating image intensity, the bottom shadow of vehicle is distinctly darker than any other areas on urban or campus road. So the bottom shadow of vehicle generally is considered as a cue for detecting vehicle. JIN et al. [13] analyzed the distribution of road surface pixels, and segmented bottom shadow of vehicle through the threshold determined by the mean and variance of the distribution. ROSEBROCK et al. [14] combined horizontal edges image with the image segmented by threshold in order to search the position of bottom shadow of vehicle. KUMAR[15] utilized the OTSU algorithm to obtain the regions including bottom shadow of vehicle. But the robustness of these algorithms is weak relatively because of another shadow sources such as trees and bridges.

The main results of this paper are shown as follows: firstly, according to the different attribution from the nearby and distant targets, a space alignment algorithm projecting radar targets onto vision image was proposed in order to provide a clue for generating ROI afterwards and reduce the sequent processing load. Secondly, a novel segmentation algorithm of bottom shadow of vehicle is presented for selecting adaptive threshold, which is robust to the simple background scenarios, complex background scenarios and illumination scenarios. Finally, with the limitation of single feature, this paper describes a vehicle detection algorithm based on fusing vision multi-features including bottom shadow obtained by above segmentation algorithm, symmetry, left and right edges, which is reliable to the different scenarios. The objective of this paper is to obtain a good performance of the vehicle detection through the collaboration of different modules composed of the different function algorithms.

1 Space alignment

The space alignment between vision and MMW radar should be performed before detecting vehicle. According to the visual perception of driver, the intelligent vehicle also has different attention on the close targets and distant targets. So the space alignment algorithm with respect to the points between the image coordinate of vision and the coordinate of MMW radar is proposed in the appropriate range related to the velocity of intelligent vehicle. In the determined range, the close regions have the smaller interval in longitudinal direction than the distant ones in order to improve the alignment precision of the close target and reduce the sequent progress load; the equable target points are gotten in suit lateral direction at the same time.

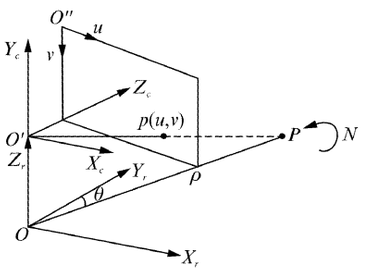

Fig. 1 The relationship of vision and MMW radar
图1 视觉和毫米波雷达的关系

The target in the coordinates of the MMW radar and vision is shown in Figure 1. The $OX_rY_rZ_r$ and $O'X_cY_cZ_c$ denote respectively the radar coordinate and camera coordinate. The $O''uv$ is image coordinate. The ρ denotes the range of target in the coordinate of MMW radar. The azimuth of the target is labeled by θ. The space transformation matrix between the (u_c, v_c) and (ρ, θ) is shown by the equation (1).

$$\begin{bmatrix} u_c \\ v_c \\ 1 \end{bmatrix} = N \begin{bmatrix} \rho\sin\theta \\ \rho\cos\theta \\ 1 \end{bmatrix} = \begin{bmatrix} n_{11} & n_{12} & n_{13} \\ n_{21} & n_{22} & n_{23} \\ n_{31} & n_{32} & n_{33} \end{bmatrix} \begin{bmatrix} \rho\sin\theta \\ \rho\cos\theta \\ 1 \end{bmatrix} \quad (1)$$

The N denotes the space transformation matrix and is estimated by the least square method including more than five corresponding points in every regions of the determined range.

The pedestrian is regarded as the reference target. With $f(u,v)$ denotes the value of pixel (u,v), the centroid of the pedestrian is computed by the equation (2).

$$u_c = \frac{\sum_u \sum_v uf(u,v)}{\sum_u \sum_v f(u,v)}, \quad v_c = \frac{\sum_u \sum_v vf(u,v)}{\sum_u \sum_v f(u,v)} \quad (2)$$

Let $U = [u_c^1 \ \cdots \ u_c^n]^T$, $V = [v_c^1 \ \cdots \ v_c^n]^T$,

$$I_{n\times 1} = [1 \quad \cdots \quad 1]^{\mathrm{T}}, P = \begin{bmatrix} \rho^1\sin\theta^1 & \rho^1\cos\theta^1 & 1 \\ \vdots & \vdots & \vdots \\ \rho^n\sin\theta^n & \rho^n\cos\theta^n & 1 \end{bmatrix}.$$

In each region of the determined range, the space transformation matrix computed by the least square method can be expressed by the equation (3).

$$N = [((PP^{\mathrm{T}})^{-1}P^{\mathrm{T}}U)^{\mathrm{T}} \quad ((PP^{\mathrm{T}})^{-1}P^{\mathrm{T}}V)^{\mathrm{T}} \quad ((PP^{\mathrm{T}})^{-1}P^{\mathrm{T}}I_{n\times 1})^{\mathrm{T}}]^{\mathrm{T}} \quad (3)$$

According to the distance and azimuth information from the MMW radar, the different space transformation matrix is applied to realize the space alignment of the vision and MMW radar. The alignment results signed by red circle are shown as figure2.

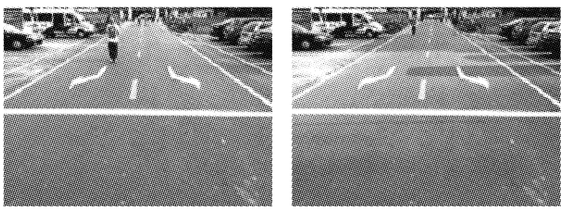

(a)　　(b)

Fig. 2　Alignment results of vision and MMW radar. (a) Result of close target. (b) Result of distant target

图 2　视觉和毫米波雷达对准结果(a)近距离目标结果(b)远距离目标结果

2　Generating ROI

In order to reduce the time of processing image, especially for large image size, the search strategy based on the space alignment result was adapted to obtain the ROI including the vehicle. It is assumed that the size of the original image is $M \times N$. Due to the error caused by the space alignment, the large width between left and right sides of ROI should be chosen. According to our experiment, the width $(2/5)N$ has been tested. The 80% of the width is considered as the height of ROI. The base of ROI is located at 50% of ROI height below the radar projection. Nevertheless, the part of ROI may lie outside the original image. In order to solve this problem, the bounds of original image are considered. In other words, the bounds of original image are regarded as the sides of ROI when ROI exceeds the original image. Figure 3 shows the generated ROI based the search strategy.

(a)　　(b)

Fig. 3　Generation of ROI (a) Original image, the red circle denotes aligned point. (b) ROI generated according to the space aligned point

图 3　产生的感兴趣区域(a)原始图像,红色圆点表示对准点(b)根据对准点生成的感兴趣区域

3　Vehicle detection

With the limitation of single vision feature, the algorithm based vision multi-features fusion is described to verify the real size of vehicle in ROI. The first specific feature is bottom shadow of vehicle[16] for determining the lower boundary. The second feature is symmetry[17]. The last feature is the left and right edges[18]. The flow chart of the algorithm is shown by figure 4.

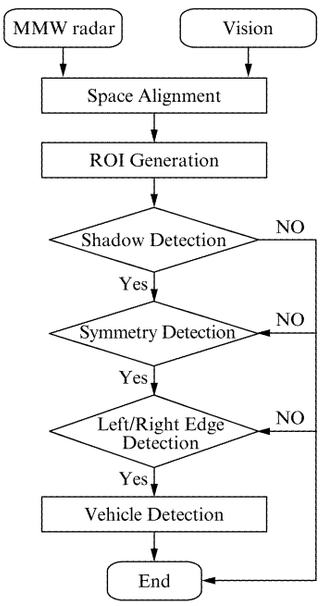

Fig. 4　The flow chart of the vehicle detection

图 4　车辆检测流程图

3.1　Bottom shadow of vehicle detection

By observing image intensity, it is found that the bottom shadow area underneath a vehicle is obviously darker than any other areas on paved road. Therefore, the bottom shadow of vehicle is usually used as an important feature for detecting vehicle. Before detecting bottom shadow of vehicle, it must be segmented accurately from the image. The OTSU[19] based multi-threshold is a good threshold method for the image of natural environment, but it has mainly two disadvantages: (1) It do not determine automatically the number of multi-thresholds. (2) The course of solving optimized multi-thresholds is time-consuming because they need to be searched among possible multi-thresholds. Generally, significant peaks of the histogram can describe the different regions in ROI. A. NAKIB et al.[20] obtained the number of multi-thresholds through the significant peaks of histogram, and computed the optimized multi-thresholds by Gaussian curve fitting and simulated annealing algorithm. However the small peak may be ignored if the valley is noticeable between adjacent peaks, and the solution of optimized multi-thresholds was complex. Particle swarm optimization (PSO) was proposed by KENNEDY et al.[21] and had advisable combination of global exploration and local exploration features during the optimization process.

MAITRA et al.[22] solved multi-thresholds through the PSO. So an improved algorithm is proposed in order to segment the bottom shadow of vehicle. The algorithm is described as follows:

1) Use the adaptive peak method to find the different regions of ROI so as to determine numbers of the multi-thresholds:

Step 1: Draw the histogram h of ROI.

Step 2: Find the local maximum set $s1$ of the histogram through the relationship between adjacent peaks.

Step 3: Find the local maximum set $s2$ like step 2.

Step 4: Set the peak threshold $th1$ and remove these elements whose value of peaks are less than $th1$, and the set $s3\_1$ is obtained from the set $s2$.

Step 5: Set the gray-level distance threshold $th2$ and remove these elements whose gray-level distances are less than $th2$, and obtain the set $s3\_2$.

Step 6: In the set $s3\_2$, set the distance threshold $th3$ between two adjacent peaks. Remove the elements which have the smaller peak if the distance of adjacent peaks is less than $th3$ and the average of the region composed of adjacent peaks is a times greater than half of summation of adjacent peaks.

According to experiment of the abundant images, the threshold $th1$, $th2$, $th3$ and a is fixed empirically. Their values respectively are $th1 = 0.05\max(h)$, $th2 = 15$, $th3 = 40$ and $a = 0.7$. The number of elements in the set s3_3 is considered as different regions in ROI. Let k denotes the number of regions, then the number of multi-thresholds segmenting ROI is k-1.

2) Solve the optical thresholds using the PSO method:

Step1: Considered k-1 as the particle dimensions.

Step2: Define and initialize the variables. The variance between different regions in OTSU method based multi-threshold is used to initialize the fitness

Step3: Adjust the position and velocity using the updated regulation of particle.

Step4: Compute the updated particle fitness: fit_s.

Step5: Compare fit_s with the optimal particle fitness: fit_pbest_s, and update fit_pbest_s and the optimal particle position, if the fit_s is greater than fit_pbest_s.

Step6: Compare fit_pbest_s with the optimal swarm fitness: fit_gbest, and update fit_gbest, the optimal swarm position: th_gbest, if the fit_pbest_s is greater than fit_gbest.

Step7: Return the th_gbest, if the iteration times reach up to maximum. Otherwise, the algorithm will come back to the Step3.

3) Segment the ROI using th_gbest and obtain the binary image through the minimal value of th_gbest.

In a simple image, the segmentation results of bottom shadow of vehicle are shown as figure 5.

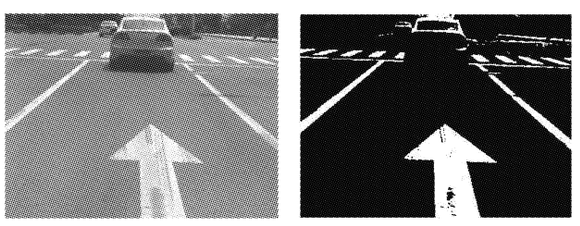

(a) (b)

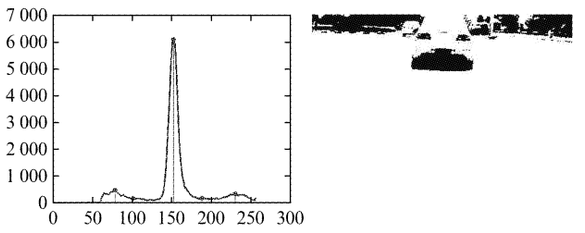

(c) (d)

Fig. 5 Segmentation of the bottom shadow. (a) Original image. (b) Shadow segmentation based on OTSU. (c) Significant peaksbased on adaptive peak method. (d) Shadow segmentation-based on the improved algorithm.

图5 车底阴影分割 (a) 原始图像 (b) 基于最大类间方差法的阴影分割 (c) 基于峰值自适应方法的重要峰值 (d) 改进算法的阴影分割

3.2 Symmetry detection

The vehicle observed from rear and frontal views is generally symmetrical. This character is considered as another cue of detecting vehicle. The symmetry of the vehicle is calculated in S-channel of HSI color space in order to avoid intensity change caused by illumination. The steps for detecting symmetry of vehicle are described as follows.

1) Convert RGB image to HSI color space.

2) In ROI, set the area based on width of bottom shadow of vehicle to compute symmetry.

3) Compute the symmetry using the equation (4) in S-channel of HSI color space.

$$sym = \arg\min(sym(u)) \quad ,(4)$$

Where $sym(u)$ can be shown as follows:

$$sym(u) = \sum_{u=u_{bl}}^{u_{br}} \sum_{v=1}^{v_b} \sum_{\Delta x=1}^{\frac{w_b}{2}} \left| \begin{matrix} S(v,u+\Delta x) \\ S(v,u-\Delta x) \end{matrix} \right| \quad ,(5)$$

where S denotes S-channel value of HSI color space, w_b is the width of the bottom shadow of vehicle, u_{bl}, u_{br} is the left and right column of the bottom shadow of vehicle, and v_b is the row of bottom shadow of vehicle.

The example is described as figure 6.

(a) (b)

Fig. 6 Location of symmetry axis of a vehicle. (a) Original image. (b) S-channel symmetry axis described by red line

图6 车辆对称轴定位(a) 原始图像(b) 红色直线表示通过S分量得到的对称轴

3.3 Left and right edge detection

The vehicle has a pair of vertical edges: left and right edges. However, it is hard to extract them because of the noise. To solve this problem, the symmetry obtained above is used to find them. Firstly, count the hor-

izontal difference values in every column and obtain the projection chart shown by figure 7. Secondly, search the maximum value on both sides of the located symmetry. Finally, define the column which has the maximum value as the left or right edge of the vehicle, and find the other edge of the vehicle according to the symmetry.

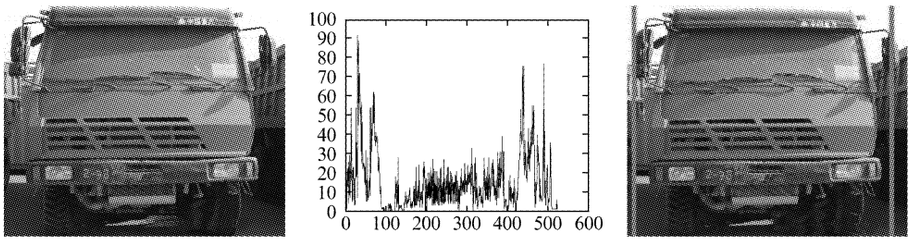

(a)　　(b)　　(c)

Fig. 7　Detection result for the left and right edges of vehicle. (a) Original image. (b) Projection chart of the vertical edges of vehicle. (c) Left and right edges indicated by the sky blue line

图 7　车辆左右边缘检测结果(a) 原始图像(b) 车辆垂直边缘投影(c) 天蓝色直线表示左右边缘

4　Experimental results analysis

In the experiment, the radar data and corresponding image sequences were obtained through the vision and MMW radar which are installed on the intelligent vehicle.

The segmentation of bottom shadow of vehicle plays an important role in the detection of vehicle. It affects directly the accuracy of sequent courses. Figure 8 shows the results of improved segmentation algorithm under different scenarios including simple background, complex background and illumination condition. To explain the efficiency of the improved segmentation algorithm of bottom shadow of vehicle, the misclassification error (Me)[23] is introduced and described by the equation (6). B_o and F_o are respectively the background and foreground area pixels of the image segmented by the manual threshold. B_T and F_T is the background and foreground area pixel of the image segmented by the different algorithms. Me represents the probability of the mistaken pixels, and its value ranges from zero to one.

$$Me = 1 - \frac{|B_o \cap B_T| + |F_o \cap F_T|}{|B_o| + |F_o|} \quad .(6)$$

Figure 9 is the statistic results of Me in different algorithms to these typical images including simple background, complex background and different illumination condition. The line with blue hexagon denotes the result of OTSU algorithm. The line with green cycle represents the result of OTSU based dual threshold algorithm. The result of improved segmentation algorithm is signed by the line with red asterisk. According to the statistic results, the average Me of different algorithm is computed and is respectively 0.541 6, 0.181 6 and 0.044 0. Therefore, the conclusion is that the improved segmentation algorithm has the better adaptability than the OTSU based dual threshold algorithm and the OTSU algorithm.

The vehicle detection algorithm has been tested in different scenarios with good results. The scenarios (SCS) are composed of the simple background (SB), the complex background (CB) and sunshine (SS). Table 1 describes the performance (PEF) of the algorithm under different scenarios. NTV denotes the number of true vehicles in image sequence. NDV is the number of detected vehicles. NSD is the number of vehicles detected successfully. DR represents the detection rate. FDR denotes the false detection rate. ADT shows the average detection time of the proposed algorithm. RADT is the average detection time of the reference method using single symmetry and the segmentation algorithm with the mean and variance of road region.

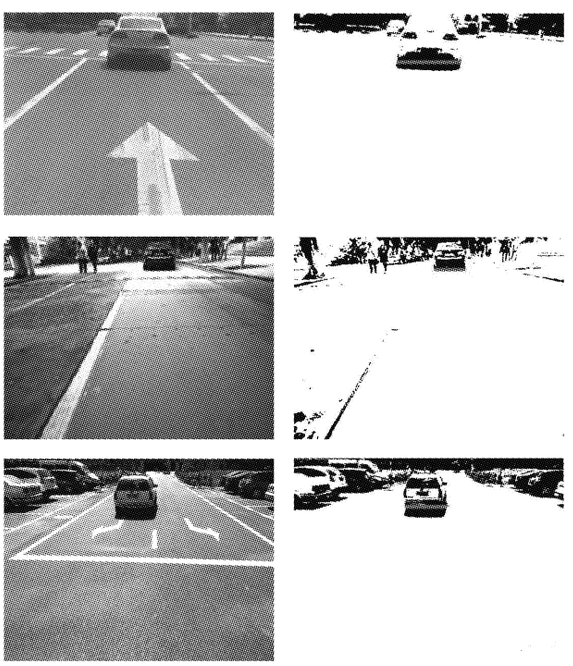

(a)　　(b)

Fig. 8　Results of bottom shadow segmentation based on the improved segmentation algorithm. (a) Original images under different scenarios. (b) Segmentation Results of bottom shadow of vehicle: the green coarse line shows the bottom shadow of vehicle

图 8　基于改进的分割算法的车底阴影分割结果(a)不同场景下的原始图像(b)车底阴影分割结果：绿色粗直线表示车底阴影

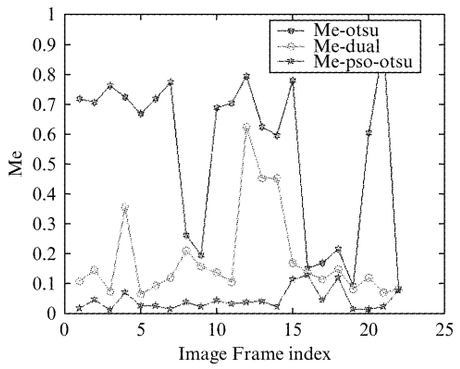

Fig. 9 Statistic results of *Me* in different algorithms
图9 不同算法下误分类误差的统计结果

Table 1 Results of different scenarios
表1 不同场景的结果

SCS / PEF	SB	CB	SS	Total
NTV	984	896	1 296	3 176
NDV	960	880	1 216	3 056
NSD	928	808	1 144	2 880
DR	94.3%	90.2%	88.3%	90,6%
FDR	3.3%	8.2%	5.9%	5.8%
ADT	0.287 5	0.615 3	0.426 9	0.440 2
RADT	0.421 3	0.684 1	0.629 7	0.578 4

The algorithm detects 90.6% of NTV, while 5.8% of the NDV are detected falsely (mainly due to complex environment and sunshine). According to these data, 3.8% of NTV are not detected, and 94.2% of NDV are detected successfully. Meanwhile, the average detection time reduces by about 24%, that is to say, the proposed algorithm not only improve the detection accuracy through introducing vision multi-features but also decrease the computational complexity. Figure 10 shows the detection results obtained in different scenarios. The red circle denotes the projection of the radar data of vehicle on the image. The green rectangle is the detection result of the proposed algorithm. The blue rectangle shows the detection result of the reference method. We can see that the proposed algorithm can well locate the vehicle.

5 Conclusions

In this paper, a vehicle detection algorithm fusing MMW radar and vision was designed. In order to get the projection of the MMW radar target on the image acquired by the vision, the space alignment algorithm was proposed according to the velocity of intelligent vehicle and the different attention on the close targets and distant targets. The different space transformation matrixes are obtained through the corresponding points between image coordinate and MMW radar coordinate. With the result of the space alignment, the search strategy is described to abstract the ROI. The ROI is used by following processes in order to reduce computing time and disturbance of natural environment. Three features of the vehicle: the bottom shadow, symmetry, and left/right edges are used to detect the preceding vehicle. Due to the significance of bottom shadow, an improved segmentation algorithm is proposed in order to accurately segment bottom shadow of vehicle; this algorithm overcomes the drawbacks of the algorithm based OSTU multi-thresholds using the adaptive peak method and PSO algorithm. The adaptive peak method mainly solves the number of different regions included in ROI. The optimal threshold is obtained through PSO algorithm. According to the area determined by the obtained bottom shadow width, the symmetry of vehicle is computed in S-channel of HSI color space. The left edge and right edge are obtained through associating the projection of horizontal difference with the located symmetry. The performance on bottom shadow segmentation and the vehicle detection algorithm fusing MMW radar and vision under different scenarios were obtained. The experiment results show that the vehicle detection algorithm gets good results with high accuracy under simple background scenarios, complex background scenarios and illumination scenarios.

The vehicle tracking based on the detection result is helpful to increase the robustness and will be introduced in future.

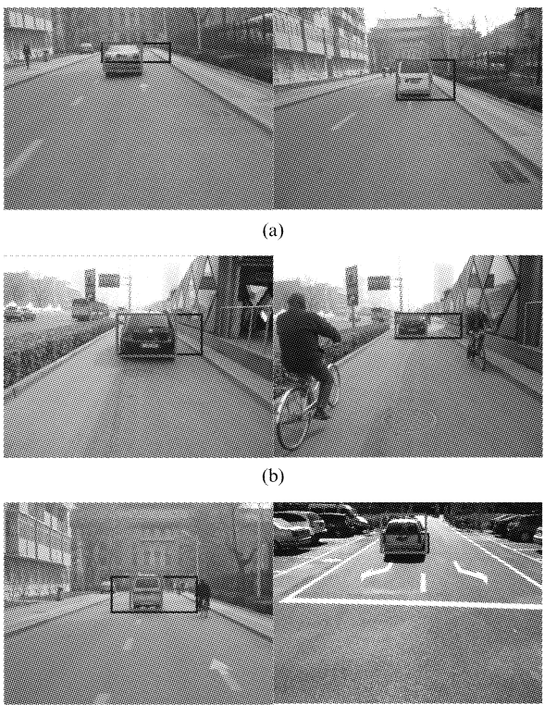

Fig. 10 Detection results of vehicle (a) simple background scenarios, (b) complex background scenarios, and (c) sunshine scenarios
图10 车辆检测结果(a)简单背景环境(b)复杂背景环境(c)光照环境

References

[1] LI Shun-Ming, SHEN Huan, MAO Jian-Guo, *et al*. Survey of intelligent vehicles development and its key supporting technologies [J]. *Transducer and Microsystems Technologies*, 2009, **28**(1): 1-4.

[2] ALESSANDRETTI G, BROGGI A, CERRI P. Vehicle and Guard Rail Detection Using Radar and Vision Data Fusion[J]. *IEEE Transactions on Intelligent Transportation Systems*, 2007, **1**(8): 95-105.

[3] SUGIMOTO S, TATEDA H, TAKAHASHI H, *et al*. Obstacle Detection Using Millimeter-wave Radar and Its Visualization on Image Sequence[C], 17th International Conference on Pattern Recognition, 2004, Cambridge. UK: IEEE, 2004: 342 - 345.

[4] LANEURIT J, BLANC C, CHAPUIS R, *et al*. Multisensorial data fusion for global vehicle and obstacles absolute positioning[C]// Intelligent Vehicles Symposium, 2003, Columbus. USA: IEEE: 138 - 143.

[5] LIU Xin, SUN Zheng-Ping, HE Han-Gen. On-road vehicle detection fusing radar and vision[C], International Conference on Vehicular Electronics and Safety, 2011, Beijing. China: IEEE: 150 - 154.

[6] WANG Tao, ZHENG Nan-Ning, XIN Jing-Min, *et al*. Integrating Millimeter Wave Radar with a Monocular Vision Sensor for On-Road Obstacle Detection Applications[J]. *Sensors*. 2011, **11**: 8992 - 9008.

[7] DENASI S, QUAGLIA G. Obstacle detection using a deformable model of vehicle[C], Intelligent Vehicles Symposium, 2001, Tokyo. Japan: IEEE: 145 - 150.

[8] FLEISCHE K R, NAGEL H H, Rath T M. 3D-model-based-vision for inner city drving scenes[C], Intellegernt Vehicles Symposium, 2002, Pairs. France: IEEE: 477 - 482.

[9] ZIEKE T, BRAUCKMANN M, SEELEN W V. Intensity and edge-based symmetry detection with an application to car-following[J]. *Imaging Understanding*. 1993, **58**(2): 177 - 190.

[10] HUANG S S, CHEN C J, HSIAO P Y, *et al*. On-board vision system for lane recognition and front-vehicle detection to enhance driver's awareness[C], International Conference on Robotics and Automation, 2004, New Orleans. USA: IEEE: 2456 - 2461.

[11] KIM S Y, OH S Y, KANG J K, *et al*. Front and Rear Vehicle Detection and Tracking in the Day and Night Times Using Vision and Sonar Sensor Fusion[C], International Conference on Intelligent Robots and Systems, 2005, Edmonton. Canada: IEEE: 2173 - 2178.

[12] TEOH S S, BRAUN T. Symmetry-based monocular vehicle detection system[J]. *Machine Vision and Application*, 2012, **23**: 831 - 842.

[13] JIN Li-Sheng, GU Bai-Yuan, WANG Rong-Ben, *et al*. Preceding Vehicle Detection Based on Multi-characteristics Fusion[C], International Conference on Vehicular Electronics and Safety, 2006, Beijing. China: IEEE: 356 - 360.

[14] ROSEBROCK D, RILK M, SPEHR J, *et al*. Using the Shadow as a Single Feature for Real-Time Monocular Vehicle Pose Determination [C], Advances in Visual Computing. 7th International Symposium, 2011, Lasvagas. USA: DBLP: 563 - 572.

[15] KUMAR C K S. A Novel Approach for Vehicle Detection for Driver Assistance[J]. *Computer Science & Information Technology*, 2012, **06**: 39 - 45.

[16] DAI Bin, FU Ya-Jun, WU Tao. A Vehicle Detection Method via Symmetry in Multi-Scale Windows[C], International Conference on Industrial Electronics and Applications, 2007, Harbin. China: IEEE: 1827 - 1831.

[17] XU Shao-Hua, ZHAO Yong, YU Chun-Yu, *et al*. Vehicle Detection Algorithm Based on Shadow Feature[C], Communication, Control and Management. International Colloquium on Computing, 2008, Guangzhou. China: 105 - 109.

[18] TSAI L W, HSIEH J W, FAN K C. Vehicle detection using normalized color and edge map[J]. *IEEE Transactions on Image Processing*, 2007, **16**(3): 850 - 864.

[19] OTSU N. A Threshold Selection Method from Gray-Level Histograms [J]. *IEEE Transactions on Systems, Man, and Cybernetics*, 1979, **9**(1): 62 - 66.

[20] NAKIB A, OULHADJ H, SIARRY P. Image histogram thresholding based on multiobjective optimization [J]. *Signal Processing*, 2007, **87**(11): 2516 - 2534.

[21] KENNEDY J, EBERHART R C. Particle swarm optimization[C], International Conference on Neural Networks, 1995, Cambridge. UK: IEEE: 1942 - 1948.

[22] MAITRA M, CHATTERJEEe A. A hybrid cooperative-comprehensive learning based PSO algorithm for image segmentation using multilevel thresholding[J]. *Expert Systems with Applications*, 2008, **34**: 1341 - 1350.

[23] NG H F. Automatic thresholding for defect detection[J]. *Pattern Recognition Letters*, 2006, **27**(14): 1644 - 1649.